ELSEVIER

Journal of Nuclear Materials 273 (1999) 139–145

journal of nuclear materials

www.elsevier.nl/locate/jnucmat

Semi-empirical models of actinide alloying

John K. Gibson [a,*], Richard G. Haire [a], Toru Ogawa [b]

[a] *Oak Ridge National Laboratory P.O. Box 2008, Oak Ridge, TN 37831-6375, USA*

[b] *Japan Atomic Energy Research Institute, Tokai-mura, Naka-gun, Ibaraki-ken, 319-11, Japan*

Received 4 December 1998; accepted 2 February 1999

Abstract

Alloys of Np have been studied less than those of the neighboring elements, U and Pu; the higher actinides have received even less attention. Recent interest in ^{237}Np, ^{241}Am and other actinide isotopes as significant, long-lived and highly radiotoxic nuclear waste components, and particularly the roles of metallic materials in new handling/separations and remediation technologies, demands that this paucity of information concerning alloy behaviors be addressed. An additional interest in these materials arises from the possibility of revealing fundamental properties and bonding interactions, which would further characterize the unique electronic structures (e.g., 5f electrons) of the actinide elements. The small empirical knowledge basis presently available for understanding and modeling the alloying behavior of Np is summarized here, with emphasis on our recent results for the Np–Am, Np–Zr and Np–Fe phase diagrams. In view of the limited experimental data base for neptunium and the transplutonium metals, the value of semi-empirical intermetallic bonding models for predicting actinide alloy thermodynamics is evaluated.

1. Introduction

The field of phase relations in alloy systems comprising actinides has recently received renewed attention, largely as a result of proposed new waste-remediation technologies which may incorporate actinides into metallic matrices. Previous investigations of the alloying behaviors of the transthorium actinides have concentrated primarily on uranium and, to a lesser extent, plutonium. The continuing accumulation of significant quantities of other actinides now demands that their alloying behaviors also be understood. In particular, ^{237}Np ($t_{1/2} = 2 \times 10^6$ yr, α-decay) and ^{241}Am ($t_{1/2} = 430$ yr, α-decay) are highly radiotoxic isotopes which are significant nuclear reactor by-products [1]. Advanced remediation schemes, which address the handling, separation/partitioning, isolation and even elimination (i.e., transmutation) of these and other nuclear materials will require characterization of new transuranium materials. Potential application areas for such actinide alloys include nuclear transmutation of waste actinides into stable isotopes via neutron irradiation, high-density metallic fuel forms, and molten salt/metal pyrochemical processing schemes [2]. Given the potential for extreme states (e.g., high-temperature) during routine or extraordinary operating circumstances, accurate knowledge or reliable predictions of materials behavior under a variety of conditions is required in order to develop safe and effective nuclear handling and remediation technologies.

The properties of these actinide materials are also of interest from a fundamental perspective. Due to their high densities, and the correspondingly small interatomic separations, metallic environments are most likely to reflect the effects of 5f electrons. Understanding the roles of 5f electrons is important since they can introduce bonding complexities which thwart the reliable modeling and prediction of alloying behavior. The effects of 5f bonding may be particularly pronounced for neptunium-containing alloys, since it has been suggested [3] that the degree of 5f bonding is maximized in this element. The chemistries and metallurgies of the light actinides (especially U, Np and Pu) are further

* Corresponding author: Tel.: +1-423 576 4291; fax: +1-423 574 4987; e-mail: gibsonjk@ornl.gov

0022-3115/99/$ – see front matter
PII: S0022-3115(99)00038-0

complicated (and rendered intriguing) by the accessibility of several oxidation states (i.e., +3 to +7) and by electronic configurations of similar energies [4].

Essential and technologically important information on the properties of alloy systems is contained in their composition–temperature phase diagrams. Establishing the existence fields of alloy phases is crucial to developing viable materials and to predicting their behaviors under variable conditions. It is generally impractical to empirically determine phase relations under all reasonable circumstances, and a variety of semi-empirical approaches have been developed to model and extrapolate what data are available. Among the more successful predictors of transition metal alloy stabilities are the models of Brewer [5,6] and Miedema [7,8]. The possible relevance of these models to understanding actinide alloying behavior is considered, with particular reference to our recent experimental results on phase relations in the following neptunium binary alloy systems: Np–Am [9], Np–Zr [10,11] and Np–Fe [12].

2. Neptunium alloy phase relations – empirical basis

Based upon the results of experimental studies, partial alloy phase diagrams have been reported for the Np–Cd [13,14], Np–U [15] and Np–Pu [16] systems. In the absence of direct experimental data, estimated diagrams have been presented for other Np binary alloy systems, such as Np–Mo [17] and Np–Cr [18]. In addition, several neptunium intermetallic compounds have been identified, including $NpPd_3$ [19], $NpAl_2$, $NpAl_3$, and $NpBe_{13}$ [20].

We recently applied high-temperature differential thermal analysis (DTA) to establish the essential features of the phase diagrams for some important Np binary alloy systems. The characteristic features reported for the Np–Am [9], Np–Zr [10,11] and Np–Fe [12] phase diagrams are summarized below.

The Np–Am system combines one metal (Np) which is characterized by substantial 5f bonding with another (Am) which exhibits little (if any) such bonding. Both of these actinides are important waste products which may be processed together. The essential conclusion from the experimental results was that the Np–Am phase diagram is characterized by immiscibility of the solid components. This finding is in contrast to the miscibility found in the Pu–Am system [21]. Ogawa [22] has suggested a possible form for the Np–Am phase diagram which is consistent with the experimental results.

The practical interest in the Np–Zr system derives from the proposed use of Zr-based alloys as advanced fuels for transmutation and other applications. Our DTA measurements on several Np–Zr alloy specimens have indicated that these two metals are largely immiscible in the solid state. This conclusion is based on the essential invariance of neptunium's transition temperatures ($\alpha \rightarrow \beta$, $\beta \rightarrow \gamma$ and melting) upon the addition of Zr. The apparent immiscible character of the Np–Zr diagram is in distinct contrast to the U–Zr [23,24] and Pu–Zr [25] systems, which are both characterized by complete high-temperature solid state miscibility, and exhibit nearly ideal elevation of the solidus/liquidus temperature upon the addition of zirconium to the actinide. It had been anticipated that the addition of zirconium to neptunium would similarly result in an elevated alloy liquidus temperature relative to pure Np°, which would be desirable in certain technological applications. The important experimental finding of a nearly invariant Np liquidus temperature (~640°C) with the addition of Zr was unexpected and potentially hindering to applications involving Np–Zr materials.

As iron is a prevalent structural material and is representative of the light transition metals, we undertook to determine the important aspects of the Np–Fe phase diagram and found it to be similar to the U–Fe and Pu–Fe diagrams [26]. Each of these three actinide-iron phase diagrams is characterized by (1) an actinide-rich (An(Fe)) eutectic ($liq = U_6Fe + UFe_2$; or $liq = An + An_6Fe$ for An = Np and Pu); (2) an iron-rich (Fe(An)) eutectic ($liq = Fe + AnFe_2$ for all three An); (3) a congruently melting compound ($AnFe_2$); (4) and an incongruently (pertitectic) melting compound (An_6Fe). Although all three diagrams have a similar form, the four important and characteristic invariant solid-liquid equilibrium temperatures, $T_{eutectic}$[An(Fe)], $T_{eutectic}$[Fe(An)], T_{melt}[$AnFe_2$] and $T_{peritectic}$[An_6Fe], are significantly different between the three systems and could not be accurately predicted for Np–Fe from those previously determined for U–Fe and Pu–Fe. The experimentally determined transition temperatures for these three An–Fe systems are shown graphically in Fig. 1. The transition temperatures for the Np–Fe system are generally intermediate between the corresponding values for the U–Fe and Pu–Fe systems, but closer to those for

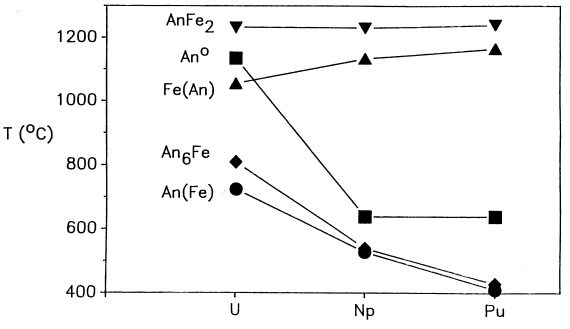

Fig. 1. Solid–liquid transition temperatures for selected pure actinide metals (An°) and An–Fe alloys: T_{melt}[An°]; T_{melt}[$AnFe_2$]; $T_{peritectic}$[An_6Fe]; $T_{eutectic}$[Fe(An)]; $T_{eutectic}$[An(Fe)].

the latter. That the melting points of the three $AnFe_2$ compounds were virtually identical (~1135°C) suggests a similar thermal stability for each. The melting points of the pure actinide elements (An°) are also included in Fig. 1 to emphasize that the nearly identical (and anomalously low) melting points of Np and Pu are substantially below that of U.

3. Application of semi-empirical predictive models

Despite recent advances in the ability to predict alloy stabilities and phase diagrams from ab initio theories [27], the application of such theories to the details of complex phase diagrams remains limited [28]. The limitations of first principles theories have proved particularly significant for alloy systems involving one or more of the d-block transition metals. Few theories have even been similarly applied to the prediction of the alloying behaviors of the f-block actinide metals, given the greater complexities and uncertainties involved with these elements. However, phenomenological models of intermetallic bonding have proved useful and successful at predicting essential aspects of transition metal alloying behavior, such as solubilities and intermediate compound formation [29]. The more versatile of these semi-empirical models invoke universal and fundamental phenomenological parameters (e.g., metallic radii, electronegativities, etc.) to correlate and predict the affinities of metallic elements for one another. Given the dearth of empirical information on phase relations in actinide alloy systems, and the particular uncertainties inherent in extrapolations to the heavier (i.e., transuranium) actinides, useful actinide alloying predictive models should be based upon such reliably relevant universal parameters. Both the Brewer [17] and Miedema [30] models have been successfully applied to the prediction of the thermochemical stabilities of a variety transition metal alloy systems, including several which incorporate actinides.

3.1. The Brewer model

The Brewer approach is essentially a Regular Solution model of alloy formation [31], with $\Delta_f G \simeq \Delta_f H - T\Delta_f^{id} S$ (i.e., $\Delta_f^{xs} S = \Delta_f S \simeq \Delta_f^{id} S \simeq 0$) and the $\Delta_f H$ estimated from intermetallic interaction parameters. Among the crucial refinements of the basic model, which allow successful application to alloy systems, is the use of inferred condensed state cohesive energies ($\Delta^* E$) in place of measured vaporization enthalpies ($\Delta_v H$) for assigning the intermetallic interaction parameters [6]. The use of $\Delta^* E$ recognizes that the actual cohesive energy, or net bonding, in a solid (or liquid) is represented by its atomization energy to the *valence bonding state* (i.e., by $\Delta^* E$), rather than to the *gaseous ground state* (i.e., by $\Delta_v H$). Experimentally measured vaporization thermodynamics refer to the final atomic ground state. In order to infer values for $\Delta^* E$ from the measured $\Delta_v H$, valence bonding state electronic configurations have been assigned to the various allotropes of the elements (including the actinides) [3] and atomic spectroscopic data have been used to establish electronic promotion energies ($\Delta^p E$) from the ground state atomic configuration to these valence bonding configuration(s) ($\Delta^* E = \Delta_v H + \Delta^p E$) [3,4,32].

The Brewer model also provides for assigning the differing contributions to the net bonding (cohesive energy) in a metal from the various types (s,p,d,f) of valence electrons [3,33]. Identification of the 5f contribution to the actinide cohesive energies is especially critical since this type of bonding, which is unique to the actinide elements, is relatively localized and directional. As a result, this bonding can be particularly disrupted by the dilution of a 5f-bonded actinide with a non-5f-bonded element; such specific bond-breaking should inhibit the miscibility between 5f-bonded actinides (e.g., U, Np, Pu) and other metals. Additional refinements incorporated into the Brewer treatment of alloying include consideration of charge-transfer (acid–base) effects in mixtures of valence electron-excess and electron-deficient metals [34].

The Brewer approach has proved useful in predicting and interpreting experimental observations on the Np–Am, Np–Zr and Np–Fe alloy systems [11]. In particular, it was suggested that the apparent immiscibility of Np with Zr may be related to the degree of 5f bonding, which is maximized at Np°, and the disruption of this bonding upon alloying. Ogawa [22] has quantitatively applied the Brewer approach to the prediction of several inter-actinide phase diagrams.

3.2. The Miedema model

The Miedema model of bonding in alloys involving transition metals, including the actinides, [7,8,28,30,35,36] invokes two elemental parameters which are fit to available empirical alloy phase relations. In its basic form the model represents the alloying enthalpy by two terms: a positive (demixing) component due to the electron density mismatch between the component metals (Δn_{WS}); and a negative (bonding) component due to electron exchange (i.e., an electronegativity effect), which is related to the difference in elemental work functions ($\Delta\phi$). The resulting form of the Miedema model for binary transition metal alloys is

$$\Delta_f H = Jf(c)[-(\Delta\phi^*)^2 + 9.4(\Delta n_{ws}^{1/3})^2]. \quad (1)$$

In Eq. (1), J is an empirical constant which may vary depending upon the nature of the alloy constituents and

$f(c)$ represents the concentration/volume dependence of the intermetallic interaction (for an alloy A_XB_{1-X} of component A in mole fraction X and component B in mole fraction $1 - X$, $f(c) = f(c^s)\cdot\{XV_A^{2/3} + (1 - X)V_B^{2/3}\}\cdot\{n_{WS}[A]^{-1/3} + n_{WS}[B]^{-1/3}\}^{-1}$ [36]).

The most accurate modeling and predictive results are generally obtained by assigning individual elemental electron densities, $n_{WS}[M]$, based upon known alloying behaviors. For example, Miedema derived $n_{WS}[Pu] = 2.99$ density units (d.u) [36] in this manner. However, for neptunium and the transplutonium actinides, insufficient experimental alloying data is available for similar derivation of reliable empirically based n_{WS}, and it is desirable to infer values of n_{WS} from fundamental elemental properties. Miedema et al. [30] have demonstrated a reliable correlation between n_{WS} and a function of the elemental volumes (V_0) and bulk moduli (B_0); this approach relates the compressibility of a metal to the electron density at the Wigner–Seitz cell boundary. We have derived n_{WS} parameters for the light actinides using the volumes given by Zachariasen [37] and the bulk moduli selected from a review by Benedict [38], using the empirical relationship:

$$n_{WS}(\text{d.u.}) \simeq 1.06\{B_0(\text{GPa})/V_0(\text{cm}^3\ \text{mol}^{-1})\}^{1/2}. \quad (2)$$

Unfortunately, the uncertainties associated with the experimental bulk moduli of the actinides, U through Am, are substantial (e.g., >10%) [38]. Our calculated $n_{WS}[An]$ are given in Table 1 along with other relevant Miedema model parameters. Whereas the n_{WS} obtained here for U (3.28 d.u.) is in reasonable agreement with that (3.44 d.u.) suggested by Miedema et al. [30], the corresponding value for Pu (2.16 d.u.) is significantly smaller than theirs (2.99 d.u.). For consistency, Miedema model calculations are made here using the $n_{WS}[An]$ values derived using Eq. (2); for plutonium, a comparison is also made with results obtained using the significantly larger value of $n_{WS}[Pu]$ from [30]. Work functions for Np and Am have not been experimentally determined but are taken to be similar to those of the neighboring actinides (see Table 1). This assumption is supported by the similarities of the Pauling electronegativities of the light actinides [39].

To assess the applicability of Eq. (1) to predicting the comparative stabilities of Np-based alloys, consideration of the signs and relative magnitudes of the calculated $\Delta_f H/J$ values is sufficient. However, it is desirable to assign a value to J and thereby report the results as approximate *absolute* alloy formation enthalpies. A recent calorimetric determination of the enthalpy of formation of UZr_2 ($\Delta_f H = -1.3$ kJ g at.$^{-1}$) [40] suggested that the absolute enthalpy calculated for this particular compound by Miedema et al. [30] may have substantially (by about three times) overestimated its stability. As UZr_2 is representative of the alloy systems being considered here, the calculated alloy stabilities were normalized to the experimental value for $\Delta_f H[UZr_2]$ (i.e., $J = 7.5$ for $\Delta_f H$ in kJ g at.$^{-1}$ using the parameter dimensions indicated in Table 1). Recognizing the substantial uncertainties in the calculated absolute enthalpy values, their relative magnitudes are emphasized here, for comparative purposes.

Miedema formation enthalpies were calculated from Eq. (1) for representative compositions in the Np–Am, Np–Zr and Np–Fe systems, for which we have experimentally determined the essential phase relations. For comparison, analogous calculations were made for the corresponding U, Pu, Am and Ta systems (Ta was included as it is similar to the light actinides in several respects, such as the magnitude of its cohesive energy, $\Delta^* E$ [3]). The results of the calculations are given in Table 2.

Formation enthalpies were calculated for both ordered MZr_2 and disordered (i.e., random solid solution) MZr phases. The similarities of the results for each MZr–MZr_2 pair illustrates that a single composition is generally sufficiently representative of the nature and degree of interaction for a given alloy pair. The calculated MZr_2 stabilities are consistent with the available experimental information: no intermediate phases (including $TaZr_2$) form in the Ta–Zr system [25]; UZr_2 [24] and $NpZr_2$ [10,11] both exist and decompose at similar

Table 1
Miedema parameters for selected metals [30,37,38]

	V (cm^3 mol^{-1})	ϕ (V)	n_{WS} (d.u.)	B_0 (GPa)
Fe	7.09	4.93	5.55	
Zr	14.00	3.45	2.80	
Ta	10.81	4.05	4.33	
U	12.5	3.90	3.28	120
Np	11.6	(3.9)	3.26	110
Pu	12.0	3.8	2.16 [a]	50
Am	17.6	(3.8)	1.60	40

[a] $n_{WS}[Pu] = 2.99$ according to Miedema [36].

Table 2
Miedema alloy formation enthalpies [a] (kJ g at.$^{-1}$)

	MZr_2 [b]	MZr [c]	MFe_2 [b]	MAm [c]
Ta	+0.8	+0.7	−5.3	+14
U	−1.3 [d]	−1.1	−3.0	+7.0
Np	−1.4	−1.2	−2.4	+6.4
Pu [e]	+0.1 {−1.0}	+0.1 {−0.8}	+7.4 {−2.3}	+1.0 {+4.9}
Am	+4.1	+3.1	+20	–

[a] Calculated using Eq. (1).
[b] Ordered intermetallic compound.
[c] Disordered alloy.
[d] Enthalpies normalized to the experimental $\Delta_f H[UZr_2]$ [40].
[e] Values in brackets obtained using $n_{WS}[Pu] = 2.99$.

temperatures (~610°C and ~550°C, respectively); and $PuZr_2$ [41] has been reported to form only when stabilized by the addition of oxygen. High-temperature measurements have further established a slight negative deviation from ideality for the U–Zr system [42] and a slight positive deviation for the Pu–Zr system [43]. The calculated Pu–Zr stabilities obtained using the value for n_{WS}[Pu] derived here from B_0[Pu] give slightly better agreement with the experimental observations than do those obtained using the value for n_{WS}[Pu] suggested by Miedema et al. [30,36]. Further assessments should aim at identifying factors which might predict those metals for which the B_0[M]-derived n_{WS}[M] values are the most applicable. According to the calculated MZr formation enthalpies, the ideal mixing entropy term (i.e., $-RT\ln X$) should be sufficient to induce high-temperature miscibility of Zr with Ta, U, Np and Pu. With the notable exception of Np [10,11], each of the other three M–Zr systems indeed forms a high-temperature body-centered-cubic solid solution phase; the model apparently fails to accurately model only Np–Zr. Compared with the lighter actinides, a lower affinity of Am for Zr is predicted; experimental results for the Am–Zr system are not available.

Results from the Miedema model suggest that a MFe_2 compound should form for M = Ta, U and Np; this is in agreement with experimental results. Furthermore, it is accurately predicted that $TaFe_2$ should be more stable than UFe_2 and $NpFe_2$; the experimental melting points are: $TaFe_2 \simeq 1775$°C; $UFe_2 \simeq NpFe_2 \simeq PuFe_2 \simeq 1235$°C [12,26]. Whereas our value for n_{WS}[Pu] fails to correctly predict $PuFe_2$ as a stable phase, the corresponding Miedema value for n_{WS}[Pu] correctly predicts that this compound should exist and exhibit a stability similar to those of the corresponding U and Np compounds. The compound $AmFe_2$ has been prepared and characterized [44] but the large positive enthalpy calculated here for it would have predicted otherwise.

The Miedema calculations for the disordered MAm phases predict that the Ta–Am, U–Am and Np–Am systems should each be characterized by immiscibility. Experimental findings for the Np–Am system [9] have confirmed this prediction. The Pu–Am phase diagram [21] is characterized by high-temperature miscibility, also in accord with the model prediction (using our value for n_{WS}[Pu]). For Pu–Am, the Miedema [36] value of n_{WS}[Pu] apparently fails to predict as accurately the observed miscibility.

The results of these illustrative examples of the application of the Miedema model to actinide systems reflect the simplifications inherent to this and similar phenomenological models when employed in their basic and most universally applicable forms. In particular, the use of *net* elemental electronegativities and electron densities does not consider the effects of differing types of bonding. For example, 5f bonding effects and multiple electronic configurations are neglected. Reflecting the similarities in the values for the volumes, electronegativities (work functions) and bulk moduli (electron densities) of U and Np (Table 1), the basic Miedema model offers little differentiation between these two actinides. Although many of the properties of U and Np are indeed similar (e.g., their volumes, as plotted in Fig. 2), significant differences are known. For example, whereas U melts at 1132°C, Np exhibits an anomalously low melting point (like Pu) of 640°C.

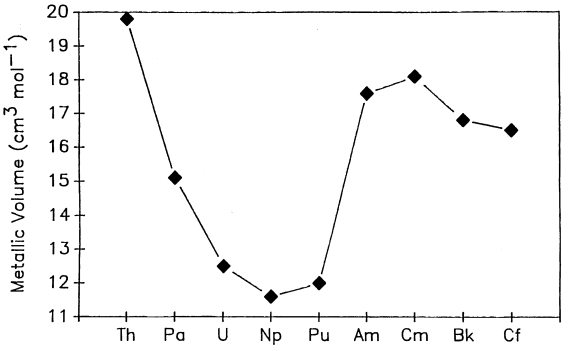

Fig. 2. Metallic volumes (V_0/cm^3 mol^{-1}) of the solid actinides [37].

It was noted that one or the other of two dissimilar values of n_{WS}[Pu] provided better predictions here, depending upon the alloy system being considered; it is doubtful whether a universal n_{WS}[Pu] can be applied, or even whether this quantity is a physically relevant intermetallic interaction parameter. The instability incorrectly predicted for $AmFe_2$ derives from the large value for the difference, Δn_{WS}[Am–Fe]. The failure of the model for the Am–Fe system may relate to a poor estimation (or irrelevance) of the n_{WS}[Am] derived from B_0[Am]. The pervasiveness of the fundamental problem of assigning relevant and physically meaningful electron density values is evident.

Since the electronegativities/work functions of the light actinides are all taken to be similar to one another, the Miedema model would suggest that variations in alloying behavior between these elements should reflect variations in electron densities. As these latter values are inferred from the bulk moduli, this latter quantity is central to the application of the model here. The actinide bulk moduli used to derive the n_{WS} given in Table 1 [38] are plotted in Fig. 3. The discrepancies in experimental B_0 values obtained by various investigators and/or differing techniques can be substantial; for example, Benedict [38] includes values for B_0[U] ranging from 100 to 143 GPa and for B_0[Pu] from 40 to 52 GPa. That the B_0 value for Pu is considerably smaller than those for U and Np is clearly evident, despite the uncertainties in the

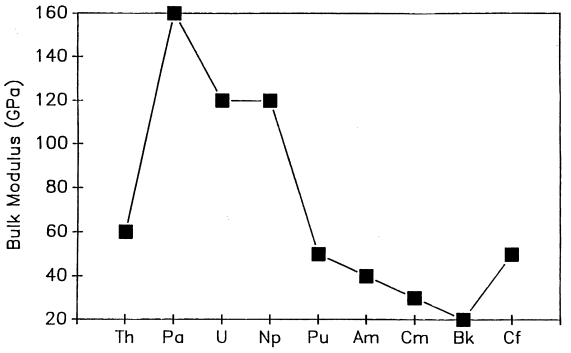

Fig. 3. Bulk moduli (B_0/GPa) of the solid actinides [38].

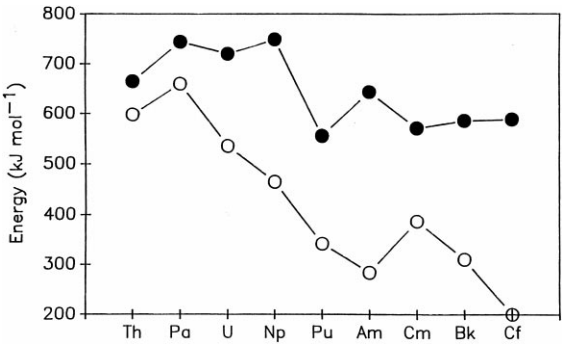

Fig. 4. Vaporization enthalpies ($\Delta_v H$/kJ mol^{-1}; open circles) and cohesive energies ($\Delta^* E$/kJ mol^{-1}; filled circles) of the solid actinides [3].

individual values. The physical origins of the anomalously small value for B_0[Pu] may not be obvious and it is not evident that it should be used to infer a correspondingly small value for n_{WS}[Pu], as was done here. A similar concern obtains for americium, and indeed the derivation of apparent n_{WS} from B_0 is possibly of questionable general validity.

4. Conclusion

The Brewer and Miedema models often predict similar alloy stabilities, particularly for alloys involving U, Np, and Pu. These comparable predictions result despite essential discrepancies in the underlying physical interpretations of the two models, the most notable contradiction perhaps being the presumed charge-transfer effects. The Brewer model, for example, would attribute the extraordinary stability of an intermetallic such as $ZrPt_3$ to a Lewis acid–base effect, involving electron transfer from Pt to Zr [34]. In distinct contrast, the Miedema model attributes the stability of such a compound to electron transfer in the opposite direction, from the less electronegative (ϕ[Zr] = 3.45 V) to the more electronegative (ϕ[Pt] = 5.65) component [30]. Quantum mechanical assessment [45] has suggested that the Brewer interpretation may be more physically accurate. That both models have proved generally applicable presumably reflects effective correlation of empirical data with relevant parameters, and not necessarily accurate representation of the details of atomistic bonding effects.

According to the basic Brewer approach, the intermetallic interaction parameters relate to the cohesive energies, $\Delta^* E$, which are plotted along with the uncorrected vaporization enthalpies, $\Delta_v H$, in Fig. 4. The large discrepancies between several of the $\Delta^* E$[An] and $\Delta_v H$[An] reflect the substantial promotion energies from the ground electronic states to the valence bonding electronic states. Focusing on the relative magnitudes of the B_0 and $\Delta^* E$ for U, Np and Pu, shown in Figs. 3 and 4, it is clear that both the Brewer ($\Delta^* E$) and Miedema (B_0) models should predict similar alloying behaviors there. Either model requires additional bonding/repulsive terms to explicitly account for more complex bonding effects, such as 5f bonding, acid-base electron exchange, variable oxidation/valence states and multiple electronic configurations.

Both Brewer [46] and Miedema [36] have demonstrated that reasonable additional considerations can be introduced into their respective models to account for the unusual behaviors of the light actinide elements. However, the appeal of the essential simplicity and clarity of the basic models is largely negated by the necessary introduction of additional secondary bonding or interaction parameters. To extrapolate the alloying behavior of Pu, for example, Miedema obtained an effective value for n_{WS}[Pu] by fitting its known phase relations; the alternative derivation of n_{WS} as a fundamental elemental parameter is more appealing and useful, especially for less well characterized elements. In summary, it is evident that the development of a substantial representative empirical data base on alloying behavior will be required for the less-common actinides (i.e., Np, Am, Cm, etc.) in order to effectively refine and confidently apply phenomenological models which may have been previously demonstrated for other transition metal alloy systems.

Acknowledgements

This work was sponsored by the Division of Chemical Sciences, Office of Science, US Department of Energy, under Contract DE-AC0596OR22464 with Lockheed Martin Energy Research Inc. and by the Japan Atomic Energy Research Institute (JAERI) under the Japan–US Actinide Program.

References

[1] G.R. Choppin, J. Rydberg, Nuclear Chemistry: Theory and Applications, Pergamon, New York, 1980, pp. 502–559.
[2] E.K. Hulet, Report of a Workshop on Transactinium Science, Report UCRL-LR-104538, Lawrence Livermore National Laboratory, CA, 1990, pp. 87–107.
[3] L. Brewer, The Cohesive Energies of the Elements, Report LBL-3720 Rev., Lawrence Berkeley Laboratory, CA 1977.
[4] L. Brewer, High Temp. Science 17 (1984) 1.
[5] L. Brewer, in: J. Stringer, R.I. Jaffe (Eds.), Phase Stability in Metals and Alloys, McGraw-Hill, New York, 1967, p. 39.
[6] L. Brewer, in: M. O'Keefe, A. Navrotsky, (Eds.), Structure and Bonding in Crystals, vol. 1, Academic Press, New York, 1981, p. 155.
[7] A.R. Miedema, J. Less-Common Met. 32 (1973) 117.
[8] A.R. Miedema, F.R. de Boer, P.F. de Châtel, J. Phys. F 3 (1973) 1558.
[9] J.K. Gibson, R.G. Haire, J. Nucl. Mater. 195 (1992) 156.
[10] J.K. Gibson, R.G. Haire, J. Nucl. Mater. 201 (1993) 225.
[11] J.K. Gibson, R.G. Haire, M.M. Gensini, T. Ogawa, J. Alloys Compounds 213&214 (1994) 106.
[12] J.K. Gibson, R.G. Haire, E.C. Beahm, M.M. Gensini, A. Maeda, T. Ogawa, J. Nucl. Mater. 211 (1994) 215.
[13] M. Krumpelt, I. Johnson, J.J. Heiberger, J. Less-Common Met. 18 (1969) 35.
[14] P. Chiotti, V.V. Akhachinskij, I. Ansara, M.H. Rand, The Chemical Thermodynamics of Actinide Elements and Compounds, Part 5, The Actinide Binary Alloys, IAEA, Vienna, 1981, pp. 205–214.
[15] R.I. Sheldon, D.E. Peterson, Bull. Alloy Phase Diag. 6 (1985) 217.
[16] R.I. Sheldon, D.E. Peterson, Bull. Alloy Phase Diag. 6 (1985) 215.
[17] L. Brewer, R.H. Lamoreaux, R. Ferro, R. Marazza, K. Girgis, Molybdenum: Physico-chemical Properties of its Compounds and Alloys, IAEA, Vienna, 1980, pp. 283–285.
[18] M. Venkatraman, J.P. Neumann, D.E. Peterson, Bull. Alloy Phase Diag. 6 (1985) 418.
[19] C. Keller, B. Erdmann, Inorg. Nucl. Chem. Lett. 7 (1971) 675.
[20] O.J.C. Runnalls, Acta Crystallogr. 7 (1954) 222.
[21] F.H. Ellinger, K.A. Johnson, V.O. Struebing, J. Nucl. Mater. 20 (1966) 83.
[22] T. Ogawa, J. Alloys Compounds 194 (1993) 1.
[23] R.I. Sheldon, D.E. Peterson, Bull. Alloy Phase Diag. 10 (1989) 165.
[24] H. Okamoto, J. Phase Equil. 13 (1992) 109.
[25] C.B. Alcock, K.T. Jacob, S. Zador, O. Kubaschewski-von-Goldbeck, H. Nowotny, K. Seifert, O. Kubaschewski, Zirconium: Physico-chemical Properties of its Compounds and Alloys, IAEA, Vienna, 1976, pp. 108–111, 122–123.
[26] O. Kubaschewski, Iron – Binary Phase Diagrams, Springer, New York, 1982, pp. 94–96, 143–146, 157–160.
[27] P.E.A. Trchi, M. Sluiter, G.M. Stocks, J. Phase Equil. 13 (1992) 391.
[28] J.C. Gachon, B.A. Selhaoui, J. Hertz, J. Phase Equil. 13 (1992) 506.
[29] K.A. Gschneidner Jr., in: L.H. Bennet (Ed.), Theory of Alloy Phase Formation, The Metallurgical Society of AIME, Warrendale, PA, 1980, pp. 1–34.
[30] F.R. de Boer, R. Boom, W.C.M. Mattens, A.R. Miedema, A.K. Niessen, Cohesion in Metals, Transition Metal Alloys, North-Holland, New York, 1988.
[31] G.N. Lewis, M. Randall, K.S. Pitzer, L. Brewer, Thermodynamics, 2nd Ed., McGraw-Hill, New York, 1961, pp. 282–290.
[32] L. Brewer, J. Opt. Soc. Am. 61 (1971) 1101.
[33] J. Kouvetakis, L. Brewer, J. Phase Equil. 14 (1993) 563.
[34] L. Brewer, P.R. Wengert, Metall. Trans. 4 (1973) 83.
[35] A.R. Miedema, P.F. de Châtel, in: L.H. Bennet (Ed.), Theory of Alloy Phase Formation, The Metallurgical Society of AIME, Warrendale, PA, 1980, p. 344.
[36] A.R. Miedema, in: H. Blank, R. Lindner (Eds.), Plutonium 1975 and Other Actinides, North-Holland, New York, 1976, pp. 3–18.
[37] W.H. Zachariasen, J. Inorg. Nucl. Chem. 35 (1973) 3487.
[38] U. Benedict, in: A.J. Freeman, G.H. Lander (Eds.), Handbook on the Physics and Chemistry of the Actinides, vol. 5, Elsevier, New York, 1987, pp. 227–269.
[39] L. Pauling, The Nature of the Chemical Bond, 3rd ed., Cornell University, New York, 1960, pp. 88–102.
[40] K. Nagarajan, R. Babu, C.K. Mathews, J. Nucl. Mater. 203 (1993) 221.
[41] J. Lauthier, N. Housseau, A. Van Craeynest, D. Calais, J. Nucl. Mater. 23 (1967) 313.
[42] A. Maeda, Y. Suzuki, T. Ohmichi, J. Alloys Compounds 179 (1992) L21.
[43] A. Maeda, Y. Suzuki, Y. Okamoto, T. Ohmichi, J. Alloys Compounds 205 (1994) 35.
[44] A.T. Aldred, B.D. Dunlap, D. Lam, G. Shenoy, in: W. Muller, R. Lindner (Eds.), Transplutonium 1975, North-Holland, Amsterdam, 1976, p. 191.
[45] D.G. Pettifor, in: H. Ehrenreich, D. Turnbull (Eds.), Solid State Physics, Advances in Research and Applications, vol. 40, Academic Press, New York, 1987, p. 43.
[46] L. Brewer, in: L.R. Morss, J. Fuger (Eds.), Transuranium Elements, A Half Century, American Chemical Society, Washington, DC, 1992, p. 138.